esBAF Facilitates Pluripotency by Conditioning the Genome for LIF/STAT3 Signaling and by Regulating Polycomb Function

Lena Ho[3,6], Erik L. Miller[4], Jehnna L. Ronan[5] , Wenqi Ho[3], Raja Jothi[2,6,*], Gerald R Crabtree[1,*]

[1]Howard Hughes Medical Institute and Departments of Developmental Biology and Pathology

[3]Program in Immunology, [4]Program in Genetics, [5]Program in Cancer Biology

Stanford University School of Medicine, Stanford, CA 94305, USA

[2] Biostatistics Branch, National Institute of Environmental Health Sciences, National Institutes of Health (NIH), 111 T.W. Alexander Drive, Research Triangle Park, NC 27709, USA

[6]These authors contributed equally to this work

*Correspondence: crabtree@stanford.edu (G.R.C.) or jothi@mail.nih.gov (R.J.)
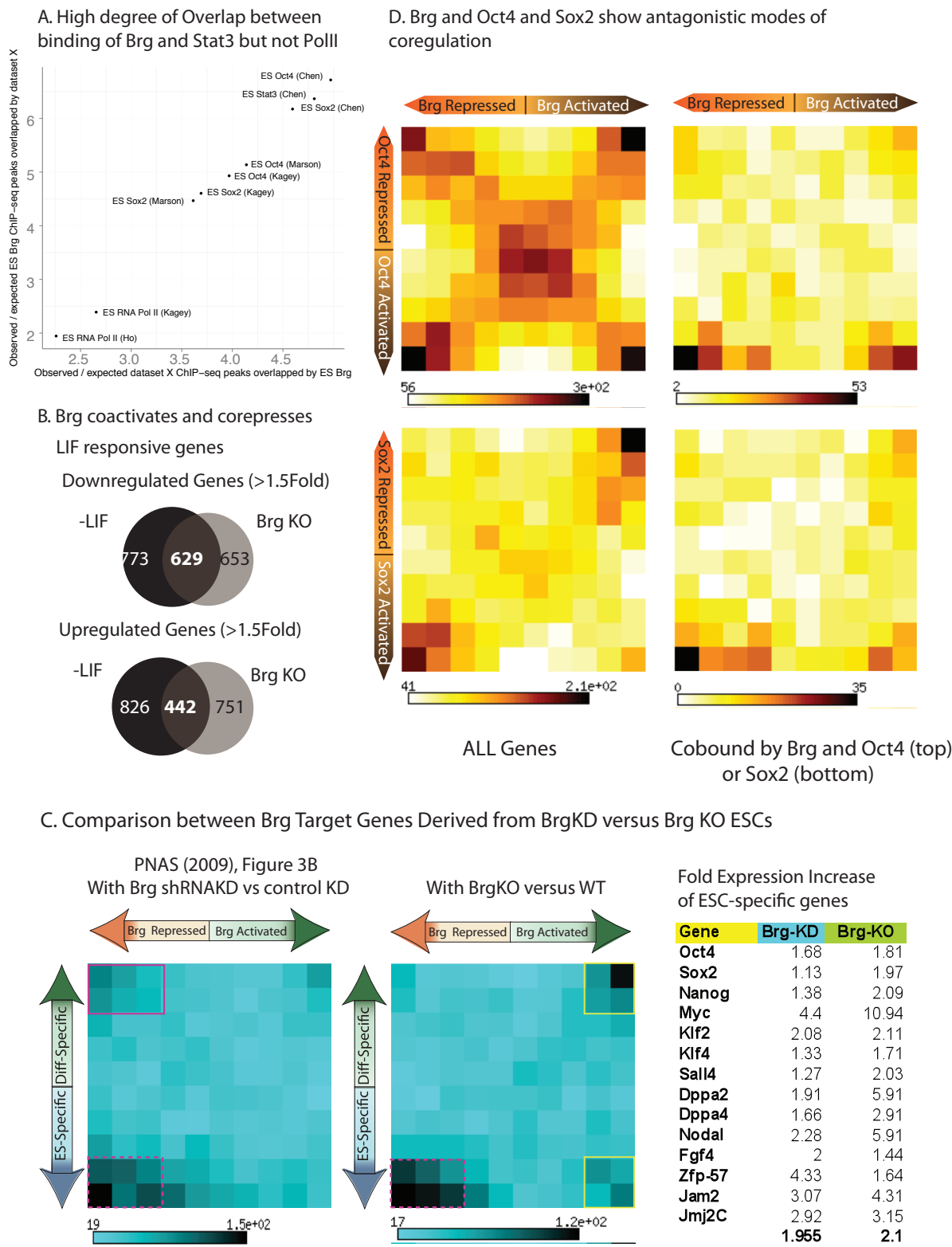
Supplemental Information
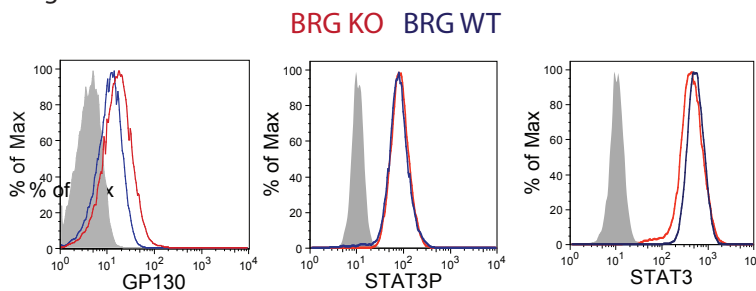
Supplemental Figures 1-9

Supplemental Tables 1-2

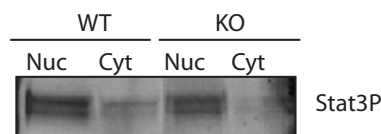Supplemental Methods

Supplemental References

Supplemental Figure 1

A. High degree of Overlap between binding of Brg and Stat3 but not PolII

Observed / expected ES Brg ChIP-seq peaks overlapped by dataset X

- ES Oct4 (Chen)
- ES Stat3 (Chen)
- ES Sox2 (Chen)
- ES Oct4 (Marson)
- ES Oct4 (Kagey)
- ES Sox2 (Marson)
- ES Sox2 (Kagey)
- ES RNA Pol II (Kagey)
- ES RNA Pol II (Ho)

Observed / expected dataset X ChIP-seq peaks overlapped by ES Brg

B. Brg coactivates and corepresses LIF responsive genes

Downregulated Genes (>1.5Fold)

-LIF 773 **629** 653 Brg KO

Upregulated Genes (>1.5Fold)

-LIF 826 **442** 751 Brg KO

D. Brg and Oct4 and Sox2 show antagonistic modes of coregulation

Brg Repressed | Brg Activated

Oct4 Repressed | Oct4 Activated

56 3e+02

Sox2 Repressed | Sox2 Activated

41 2.1e+02

Brg Repressed | Brg Activated

2 53

0 35

ALL Genes

Cobound by Brg and Oct4 (top) or Sox2 (bottom)

C. Comparison between Brg Target Genes Derived from BrgKD versus Brg KO ESCs

PNAS (2009), Figure 3B
With Brg shRNAKD vs control KD

Brg Repressed | Brg Activated

ES-Specific | Diff-Specific

19 1.5e+02

With BrgKO versus WT

Brg Repressed | Brg Activated

ES-Specific | Diff-Specific

17 1.2e+02

Fold Expression Increase of ESC-specific genes

Gene	Brg-KD	Brg-KO
Oct4	1.68	1.81
Sox2	1.13	1.97
Nanog	1.38	2.09
Myc	4.4	10.94
Klf2	2.08	2.11
Klf4	1.33	1.71
Sall4	1.27	2.03
Dppa2	1.91	5.91
Dppa4	1.66	2.91
Nodal	2.28	5.91
Fgf4	2	1.44
Zfp-57	4.33	1.64
Jam2	3.07	4.31
Jmj2C	2.92	3.15
	1.955	**2.1**

E. Exp ression of LIF Signaling Components is Not Impaired in BrgKO ESCs

G. BrgKO ESC Transcriptome Does Not Reflect Differentiation

BRG KO   BRG WT

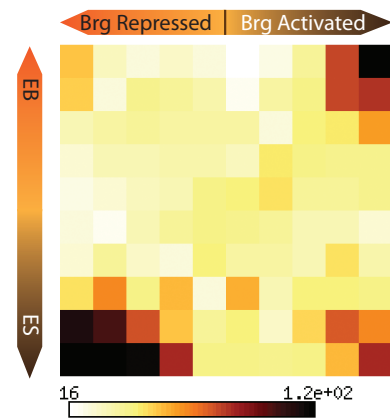F. Nuclear Localization of Phosphorylated Stat3 Is Not Impaired In BrgKO ESCs

Figure S1 Gene Expression Changes in BrgKO ESCs

A) The observed/expected ratio was calculated for each pair of factors, Brg and Stat3 or Brg and RNA Polymerase II.

B) Overlap between down- and up-regulated genes from microarray studies of BrgKO ESCs (versus WT ESCs) and 48hr LIF-starved ESCs (versus WT ESCs). Genes are defined as up or downregulated if their fold change exceeds 1.5 and is statistically significant (FDR<0.05) compared to WT ESCs.

C) 2D matrices and heatmaps depicting gene expression changes in shRNA-mediated Brg knockdown ESCs and compared to control knockdown ESCs (left panel) or BrgKO versus WT ESCs (middle panel) for all Brg-bound genes. Axes indicate degree of fold change, from nil (middle of axis) to greater than 1.5-fold downregulated (right outermost square) or upregulated (left outermost square); (right panel) Table documenting the fold upregulation of key ESC-specific pluripotency genes in Brg knockdown and Brg KO ESCs.

D) 2D matrix depicting direction and magnitude of gene expression changes for Brg KO ESCs (x-axis) compared to gene expression changes in ESCs depleted of Oct4[1, 2] (top) or Sox2[21](bottom) (y-axis). Axes are divided into 10 bins containing equal number of genes ranging from ~1.5 median fold upregulated (left or top) to ~1.5 median fold downregulated (right or bottom) in experiments compared to WT. The color intensity of each square depicts the number of genes in each square, as defined by the color bar below each plot. 2 matrices on the left contain all genes present on the microarray data used for this analysis, while the two matrices on the right are further filtered for direct targets and Oct4 or Stat3 based on binding of these factors within 5Kb upstream of the transcription start site of a gene.

E) Intracellular staining and flow cytometry of gp130, STAT3 and STAT3-pT705 in BrgWT (blue) and BrgKO ESCs (red). Grey=background control.

F) Levels of STAT3-pT705 in nuclear and cytoplasmic fractions of Brg WT and KO ESCs cultured in the presence of LIF.

G) 2D matrix depicting direction and magnitude of gene expression changes for Brg KO ESCs (x-axis) compared to gene expression changes in differentiated embroid bodies or EBs (y-axis) (EB=genes upregulated in EBs; ES=genes downregulated in EBs, or ES-specific genes) Axes are divided into 10 bins containing equal number of genes ranging from ~1.5 median fold upregulated (left or top) to ~1.5 median fold downregulated (right or bottom) in experiments compared to WT. This matrix shows that BrgKO ESCs do not show overt differentiation since their gene expression profile does have a positive correlation with that of ESCs undergoing spontaneous differentiation (i.e. EB formation).

Supplemental Figure 2

A. LIF Responsive Transcription is Impaired in the Absence of Brg
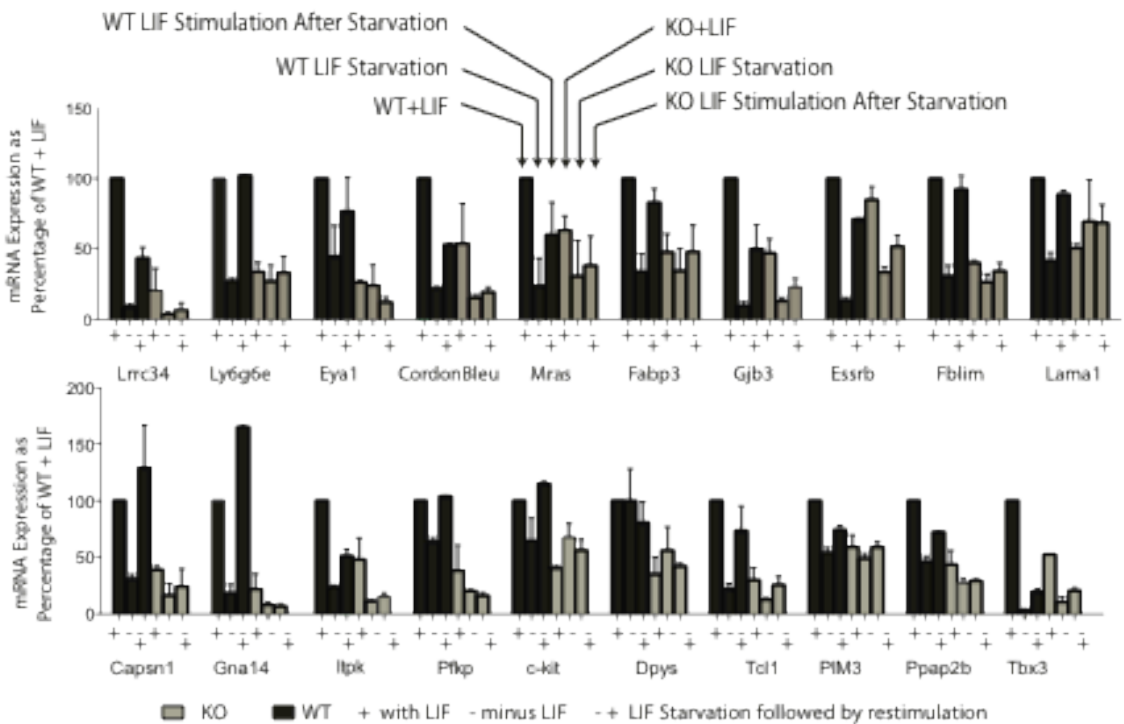
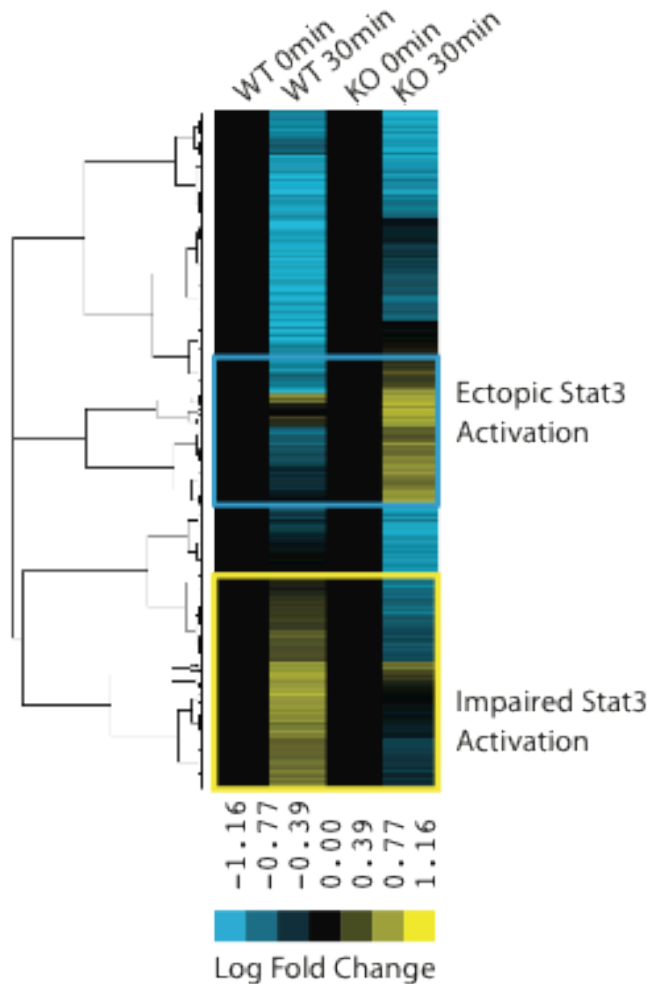B. Brg is Required for ES-Specific Stat3 Transcriptome

Figure S2. LIF-responsive, STAT3-dependent transcription in ESCs is Brg-Dependent

A)The transcript levels of Brg and STAT3-dependent cobound coactivated genes (i.e. BR1 genes) were measured in BrgWT and BrgKO (grey) ESCs by QPCR in the presence of LIF (+), after 24hours of LIF starvation (-) followed by LIF stimuation for 24hours. Transcript levels are expressed as a percentage of that in WT ESCs grown in the presence of LIF. B) WT and BrgKO ESCs were starved from LIF for 18hours, followed by 30 minutes of LIF stimulation. Microarray analysis of all four samples (with 1 replicate each) was performed. LIF stimulated samples were compared with the respective LIF-starved samples (i.e. WT or KO, representing basal level of LIF signagling) and the fold change of each gene was calculated (LIF restimulation/LIF starved). The color bar depicts the fold change of each gene compared to the baseline. We performed hierachical clustering with Java Treeview 1 to visualize the data.

Supplemental Figure 3

A. New Stat3 Sites Are Acquired in BrgKO ESCs

B. esBAF Recruitment is Modestly Dependent on STAT3

C. Stat3ER is activated by 4-OHT- and is LIF-independent

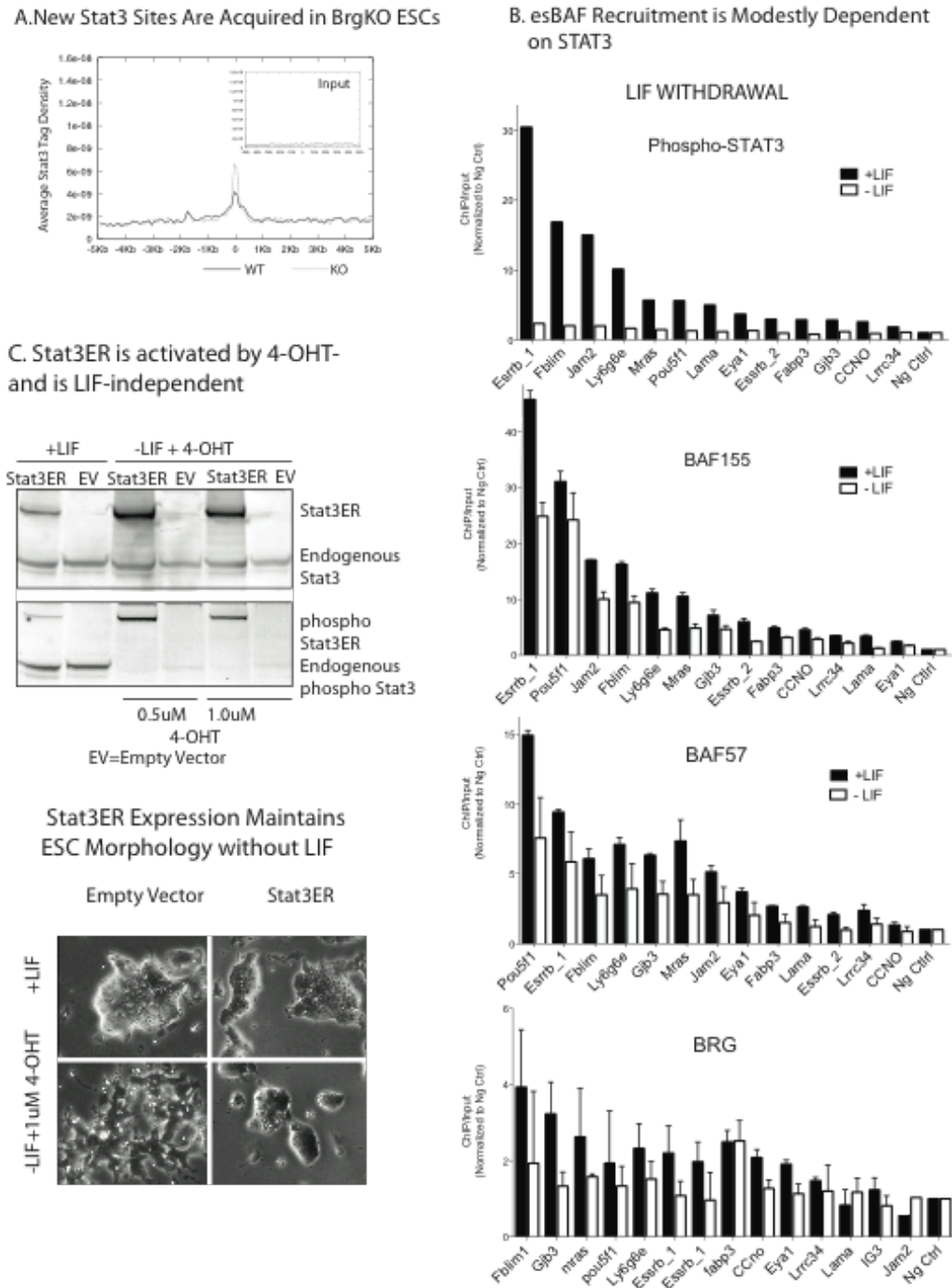Stat3ER Expression Maintains ESC Morphology without LIF

Figure S3. Enforced STAT3 nuclear localization in Brg f/f ESCs

A) Novel STAT3 Sites are Acquired in BrgKO ESCs. Average tag density plots of STAT3 ChIP Seq signals in Brg WT and Brg KO ESCs at sites where STAT3 binds in BrgKO ESCs but not BrgWT ESCs, i.e. novel STAT3 sites in ESCs in the absence of Brg.

B) ChIP assays of phospho-Stat3 and esBAF components BAF57, BAF155 and Brg in ESCs grown in the presence of LIF or in the absence of LIF for 24 hours, which is sufficient to remove STAT3 from its target sites. Y-axis represents ChIP/Input ratio for

each region, normalized with the ratio a negative intergenic region (Ng ctrl). *Pou5f1* is used here as a positive control for ChIP of esBAF components, but is not classified as a Brg and STAT3-coactivated gene. Error bars = SEM of 2 independent experiments.

C) Top: Levels of total and phosphorylated endogenous STAT3 and transgenic STAT3ER fusion protein in Brg[cond];STAT3ER (STAT3ER) or Brg[cond];Empty Vector (EV) ESCs grown in the presence of LIF, or in LIF-free media containing 4-OHT, which induces nuclear translocation and activation of STAT3 and also *Brg* deletion at the same time. Bottom: Morphology of Brg[cond];STAT3ER and Brg[cond];EV cells grown in the presence of LIF or in LIF-free media containing 4-OHT
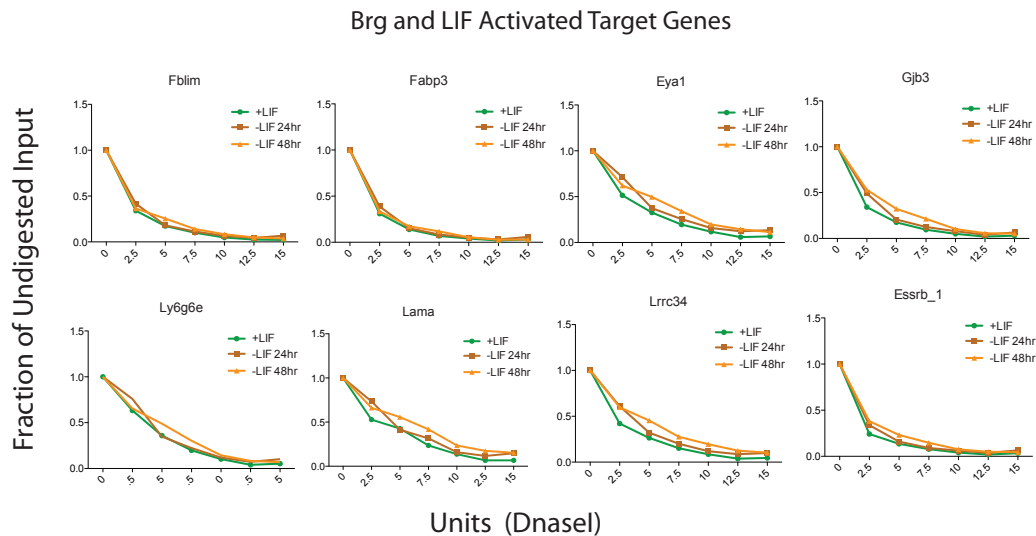
Supplemental Figure 4
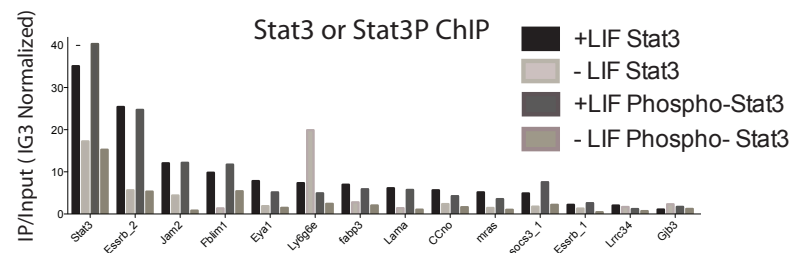
A. Overlap of Brg Sites with DnaseI Hypersensitive Sites
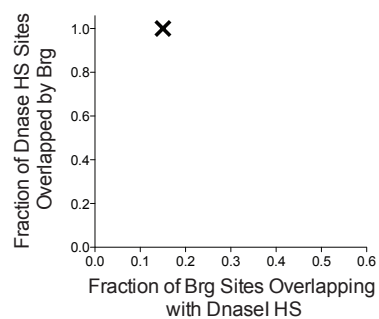
B. Decreased Accessibility of Stat3 Target Sites to Nuclease in the Absence of Brg

Brg Dependent Stat3 Sites

Brg Independent Stat3 Sites
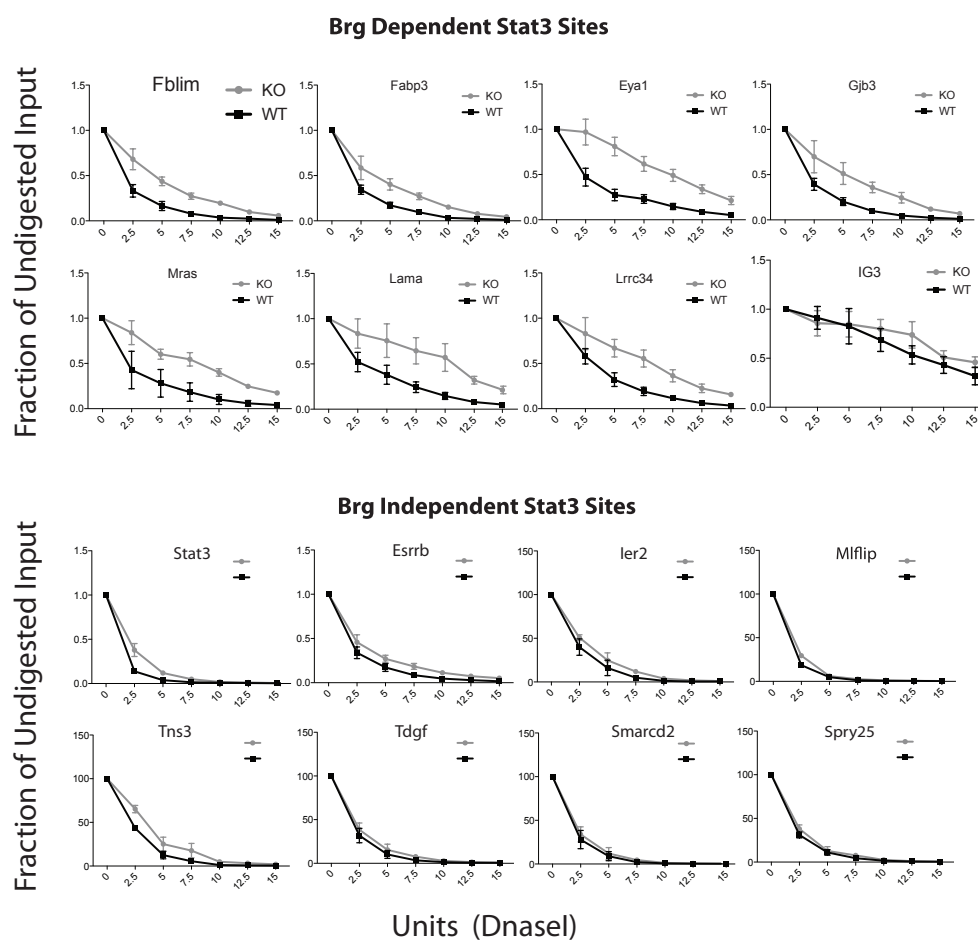
C. Stat3 Target Sitse DNaseI Accessibility Following LIF Withdrawal

Brg and LIF Activated Target Genes

Stat3 and Stat3P Occupancy Following LIF Withdrawal

Figure S4. Accessibility of STAT3 target sites in ESCs is Brg-Dependent

A) DnaseI hypersensitive sites (HS) from Schnetz et al. 2 were compared with Brg binding regions to measure the degree of physical overlap between them. Y-axis indicates the fraction of Brg sites that are also DNaseI HS sites, while x-axis indicates the fraction of DnaseI HS sites that are also Brg binding regions.

B) DnaseI hypersensitive assay of STAT3 sites targeting BR1 genes that are Brg-dependent or randomly chosen Brg-independent sites in BrgWT versus BrgKO (grey) ESCs. IG3 is a negative intergenic control that does not bind STAT3. Error bars represent SEM of two independent experiments.

C) (Top) DnaseI hypersensitive assay of Brg-dependent STAT3 sites in WT +LIF, and following 24hours and 48hours of LIF starvation. (Bottom) STAT3 and STAT3-pT705 ChIP assays confirming that STAT3 and STAT3P levels are decreased at the Brg-
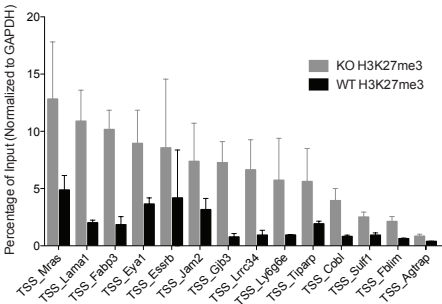
dependent sites probed with DnaseI assay. Results are expressed as percentage of ChIP/Input nomralized to ChIP/Input ratio of a negative control region IG3
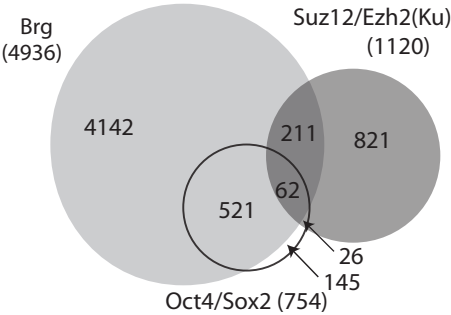
Supplemental Figure 5

A. Activating Marks H3K4ME3 and H4Ac At Stat3 Target Genes 72 hours POst Brg Deletion
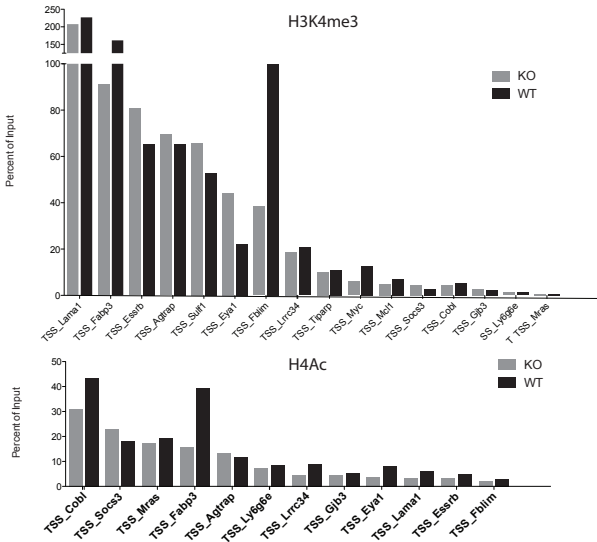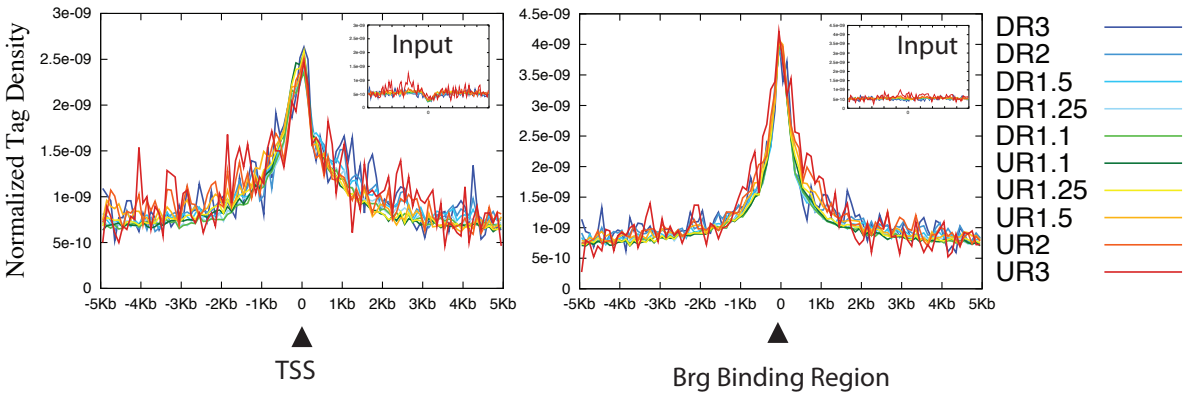

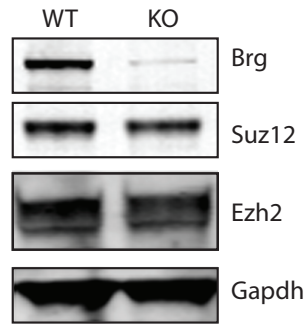## B. Increase of H3K27me3 mark at TSS of Stat3 Target Genes

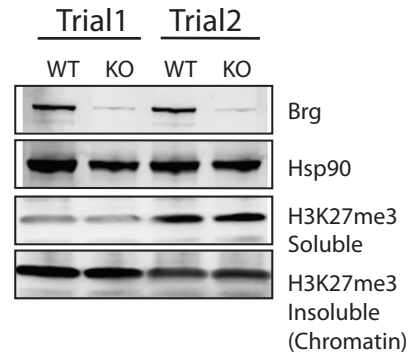## C. Overlap of Suz12/Ezh2, Oct4/Sox2 and Brg Target Genes

D. Brg Binding Profile over TSS and Brg Binding Site of Brg Target genes
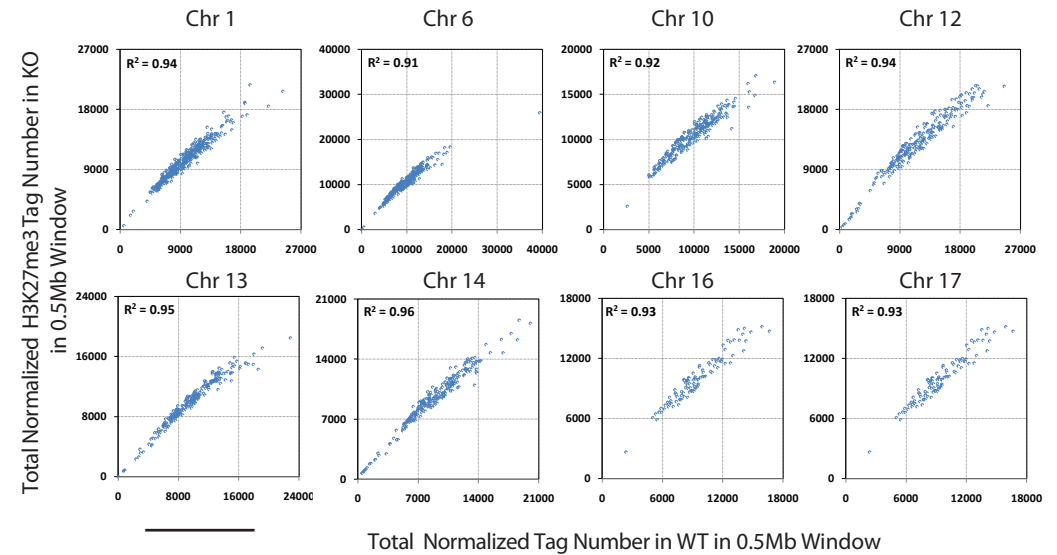
E. PRC2 Protein Levels in BrgKO ESCs

WT	KO	
		Brg
		Suz12
		Ezh2
		Gapdh

F. Global Levels of H3K27me3 Does not Increase in BrgKO ESCs

Trial1		Trial2		
WT	KO	WT	KO	
				Brg
				Hsp90
				H3K27me3 Soluble
				H3K27me3 Insoluble (Chromatin)

G. No Global Changes in H3K27me3 In BrgKO ESCs

Chr 1 — $R^2 = 0.94$
Chr 6 — $R^2 = 0.91$
Chr 10 — $R^2 = 0.92$
Chr 12 — $R^2 = 0.94$
Chr 13 — $R^2 = 0.95$
Chr 14 — $R^2 = 0.96$
Chr 16 — $R^2 = 0.93$
Chr 17 — $R^2 = 0.93$

Total Normalized H3K27me3 Tag Number in KO in 0.5Mb Window

Total Normalized Tag Number in WT in 0.5Mb Window

H. Transcriptional Derepression Of Brg Targets in Hox Cluster

mRNA Expression Units (Hsp90 Normalized)

KO, WT

Hoxa5, Hoxa7, Hoxa9, Hoxb13, Hoxd9, Hoxd11, Hoxd10, Hoxd13

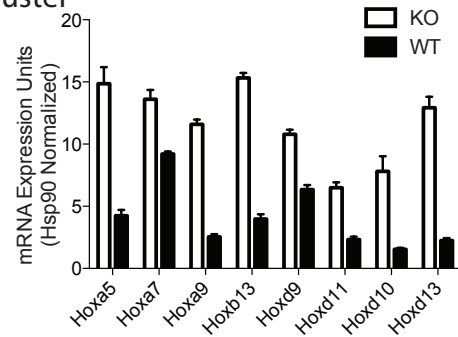## Figure S5. Brg Deletion Results in PRC2-Dependent Gene Repression

A) ChIP-qPCR of activating histone modifications H3K4me3 and acetylated H4 (H4Ac) in Brg WT (black) versus Brg KO ESCs (KO), 72 hours after induction of *Brg* deletion. Results are representative of 3 indepenent experiments, and are expressed as ChIP/Input normalized to the ratio of an intergenic control that has very low levels of both modifications.

B) H3K27me3 ChIP at the transcriptional start site of representative Brg- and LIF coactivated genes in WT and BrgKO ESCs. Y-axis represents ChIP/Input ratio for each region, normalized with the ratio at the *GAPDH* promoter. Error bars = SEM of 3 independent experiments.

C) Overlap of Brg 14, Suz12/Ezh2 (PRC2) 27 and Oct4 and Sox2 target genes 26. Target gene definition is binding of a factor within -5Kb of TSS to transcription end site, TES. P-values from hypergeometric distribution of significance of overlap are: 1.77E-201 (Brg vs Oct4/Sox2); 0.14 (Brg vs PRC2); 3.85E-10 (Oct4/Sox2 vs PRC2).

D) Plots depicting the occupancy of Brg over TSS and Brg binding regions for the categories of Brg target genes used in Figure 4. Y-axis represents average normalized tag density of Brg for each group, anad x-axis measures the distance from the TSS or Brg binding site of a Brg target gene. Normalized tag density of input is shown in inset within each panel.

E) Western blot of PRC2 components Suz12 and Ezh2 in BrgWT and BrgKO ESCs, with GAPDH as a loading control. Full length blots are presented in Figure S9d.

F) Global levels of trimethylated H3K27 (H3K27me3) in soluble and chromatin fractions of BrgWT and BrgKO ESCs. Hsp90 is used as a loading control. Full length blots are presented in Figure S9e.

G) Scatter plots of H3K27me3 levels on representative chromosomes. Each point represents the total number of tags in a particular 0.5Mb window in Brg KO (y-axis) and the total number of tags in the corresponding 0.5Mb window in Brg WT (x-axis) ESCs. If a point falls on the diagonal of the plot, there is a similar overall tag number in that window in Brg KO ESCs compared to WT. Since the trendline of each plot falls on the diagonal, there is no overall change in tag numbers derived from ChIP-seq of H3K27me3 in KO versus WT ESCs.

H) mRNA levels of *Hox* genes in BrgWT and BrgKO ESCs, normalized to *Hsp90* mRNA levels. Error bars= SEM of 3 independent experiments.

Supplemental Figure 6

A. Brg Occupancy over TSS and Stat3 Site of Brg/Stat3 CoActivated Targets
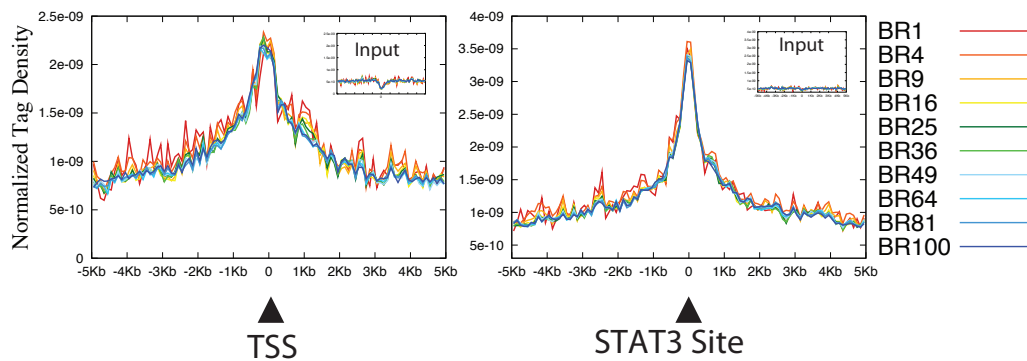
B. TimeCourse Analysis of H3k27me3 versus Transcript Levels
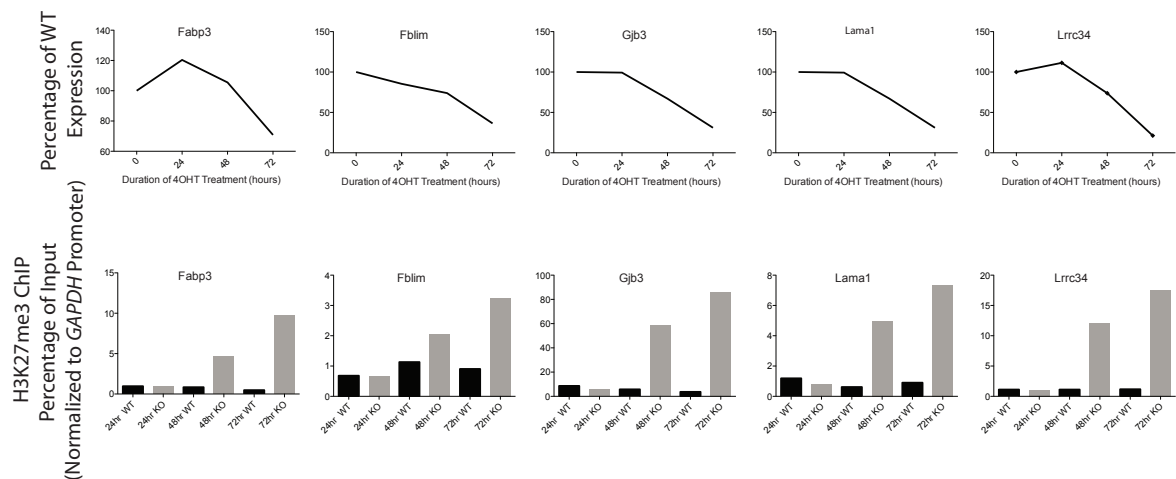
C. LIF Withdrawal Does Not Cause Increase of H3K27me3
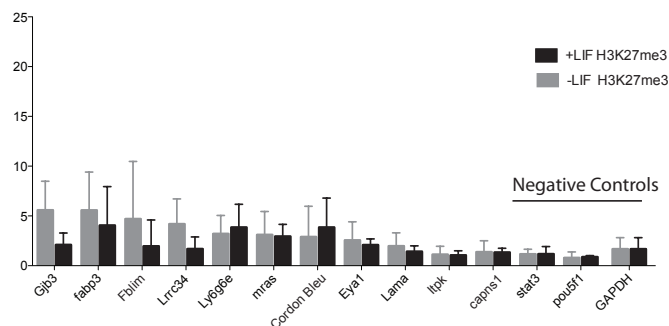
Figure S6. Dynamics of H3K27me3 Increase At Stat3 Target Genes

A) Plots depicting the occupancy of Brg over TSS and Stat3 binding regions for the categories of Brg/Stat3 cotarget genes used in Figure 6a. Y-axis represents average normalized tag density of Brg for each group, anad x-axis measures the distance from the TSS or Brg binding site of a Brg target gene. Normalized tag density of input is shown in inset within each panel.

B) H3K27me3 Increase Is Concurrent with Transcriptional Downregulation (Top)
Timecourse analysis of transcript levels of Brg-dependent STAT3 genes (expressed as
percentage of time 0) following initiation of 4-OHT treatment (i.e. *Brg* deletion).
(Bottom) Timecoures analysis of H3K27me3 levels at the STAT3 binding sites of the
same genes by ChIP analysis. Results are expressed as percentage of ChIP/Input
normalized to the ChIP/Input ratio of a negative control GAPDH promoter. Black = Brg
WT; Grey= BrgKO.

C) LIF Withdrawal does not increase H3K27me3 at STAT3 target genes. H3K27me3
levels at representative Brg-dependent STAT3 sites in WT ESCs grown in the presence
of LIF (black) and following 48 hours of LIF withdrawal (grey). Results are expressed as
percentage of ChIP/Input normalized to the ChIP/Input ratio of a negative control
GAPDH promoter, and represent mean and SEM of 3 biological replicates.

Supplemental Figure 7

Representative Screen Shots of BR1 Genes With INcreased H3K27me3
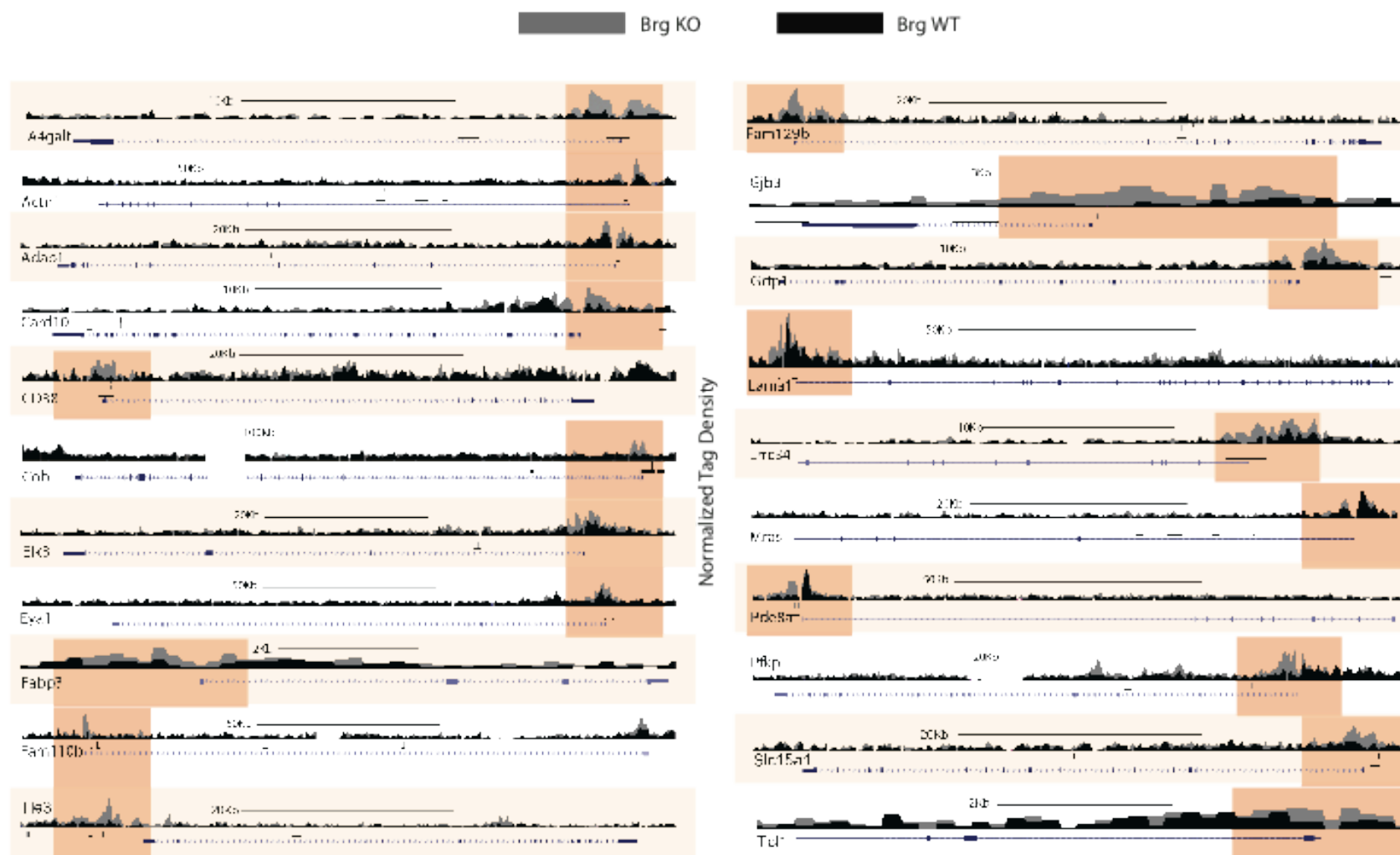
Figure S7 Browser shots from UCSC Genome Browser of representative BR1 genes with increase in H3K27me3 in BrgKO ESCs.

Grey trace represents H3K27me3 profile in KO ESCs, and black trace represents H3K27me3 profile in WT ESCs. Orange boxes are positioned to highlight the region of H3K27me3 increase in Brg KO ESCs

Supplemental Figure 8

A. PRC2 Occupancy Does Not Increase with LIF Withdrawal

B. Suz12 shRNA-mediated Knockdown in WT ESCs
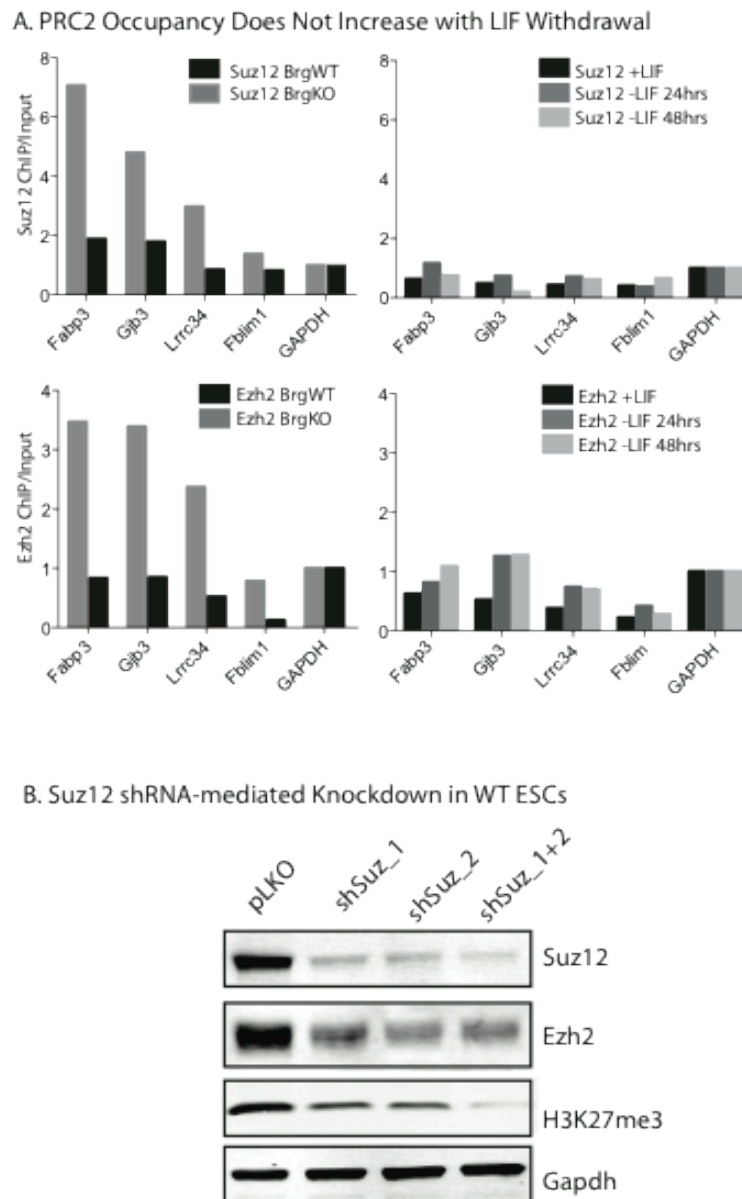
Figure S8 Suz12 Knockdown in BrgKO ESCs

A) Comparison of Suz12 and Ezh2 levels at representative Brg-dependent STAT3 genes by ChIP assay in BrgWT vs BrgKO ESCs (left) and in WT ESCS grown in LIF and without LIF for 24 and 48 hours (right). Results are expressed as percentage of ChIP/Input normalized to the ChIP/Input ratio of a negative control GAPDH promoter and are representative of 3 independent experiments.

B) Protein levels of PRC2 components Suz12 and Ezh2 following either control or Suz12 shRNA-mediated knockdown. Two distinct Suz12 knockdown constructs are utilized, both separately and together. Knockdown constructs were delivered via lentiviral

transduction and protein levels were measured 4 days post-infection and puromycin selection. Full length blots are presented in Figure S9f.

Supplementary Figure 9

A. Uncropped Western Blots for Figure 1A
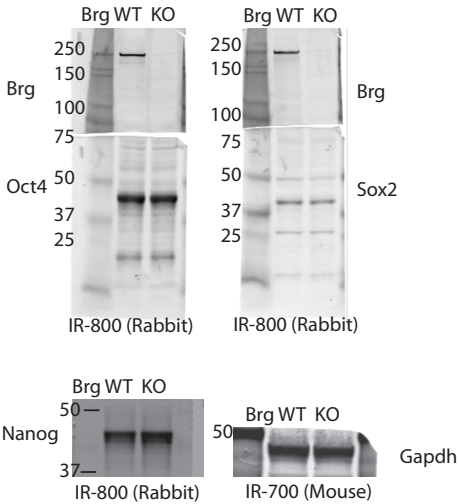
Brg WT KO
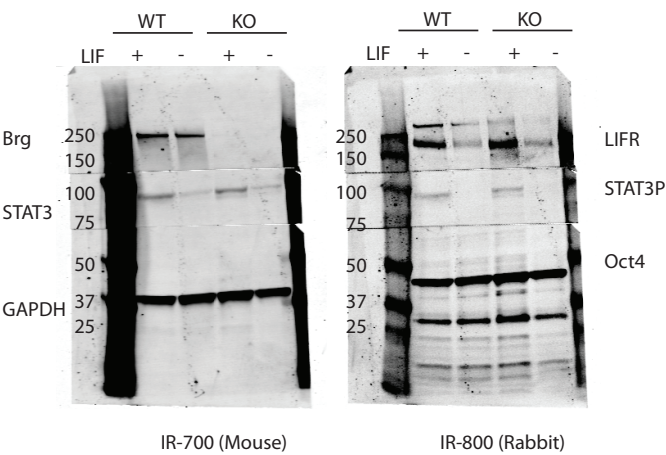
Brg

| 250 |
| 150 |
| 100 |
| 75 |

Oct4 50

37

25

IR-800 (Rabbit)

Brg WT KO

| 250 |
| 150 |
| 100 |
| 75 |

50

37

25

Brg

Sox2

IR-800 (Rabbit)

Brg WT KO

Nanog

50 —

37 —

IR-800 (Rabbit)

Brg WT KO

50 —

Gapdh

IR-700 (Mouse)

B. Uncropped Western Blots for Figure 1D

WT   KO

LIF + - + -

Brg   250
      150

STAT3 100
      75

      50

GAPDH 37
      25

IR-700 (Mouse)

WT   KO

LIF + - + -

250   LIFR
150

100   STAT3P

75

50   Oct4

37
25

IR-800 (Rabbit)

C. Uncropped Western Blots for Figure 1E

IR-700 (Mouse)   IR-800 (Rabbit)

BrgWT

STAT3

GAPDH

| 250 |
| 150 |
| 100 |
| 75 |
| 50 |
| 37 |
| 25 |

STAT3Tyr705

Oct4

BrgKO

STAT3

GAPDH

IR-800 (Rabbit)

STAT3Tyr705

Oct4

+ - +5 +15 +60 +180   + - +5 +15 +60 +180

LIF Addition in Media

D. Uncropped Western Blots for Figure S5E

IR-800 (Rabbit)

IR-700 (Mouse)

E. Uncropped Western Blots for Figure S5F

IR-800 (Rabbit)

IR-700 (Mouse)

F. Uncropped Western Blots for Figure S8B

IR-800 (Rabbit)

IR-700 (Mouse)
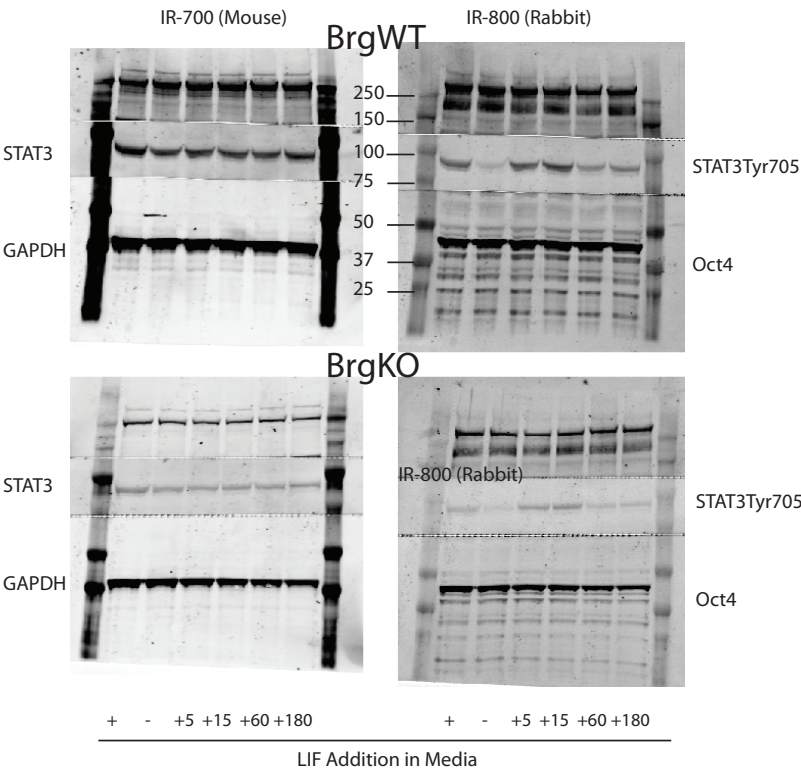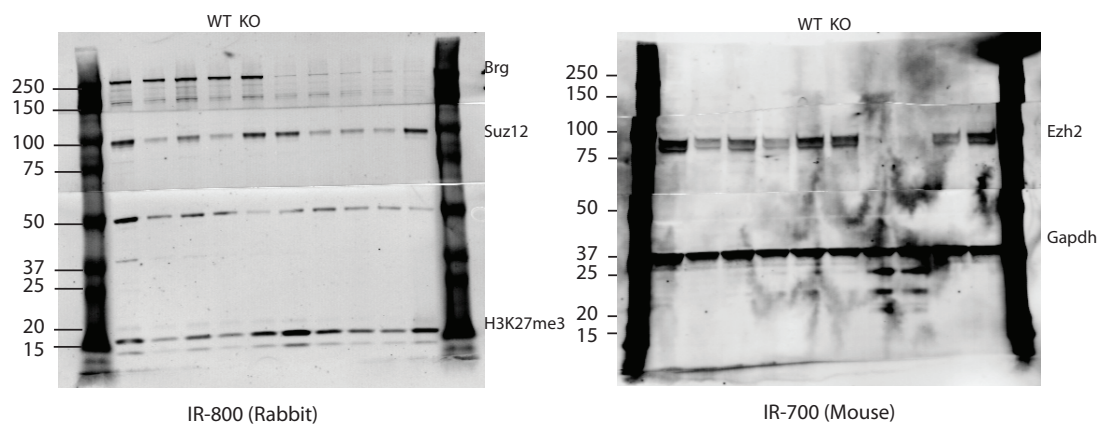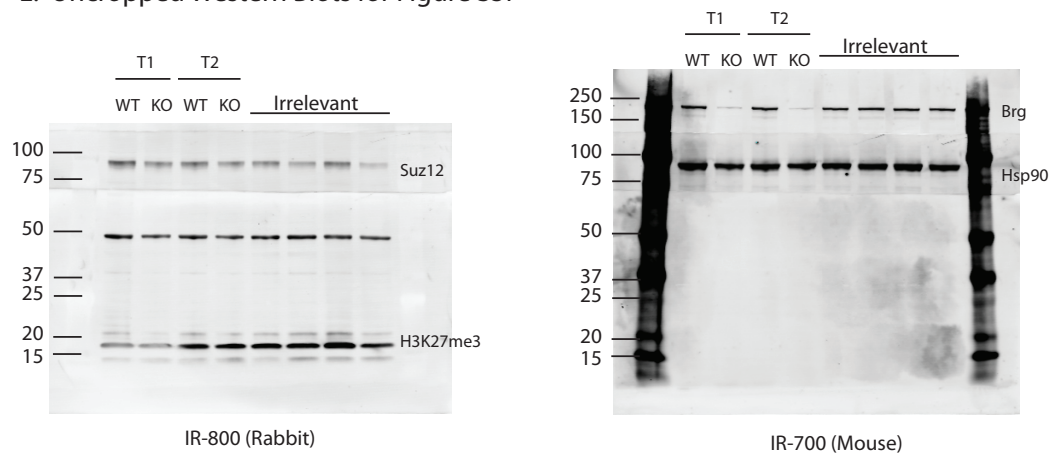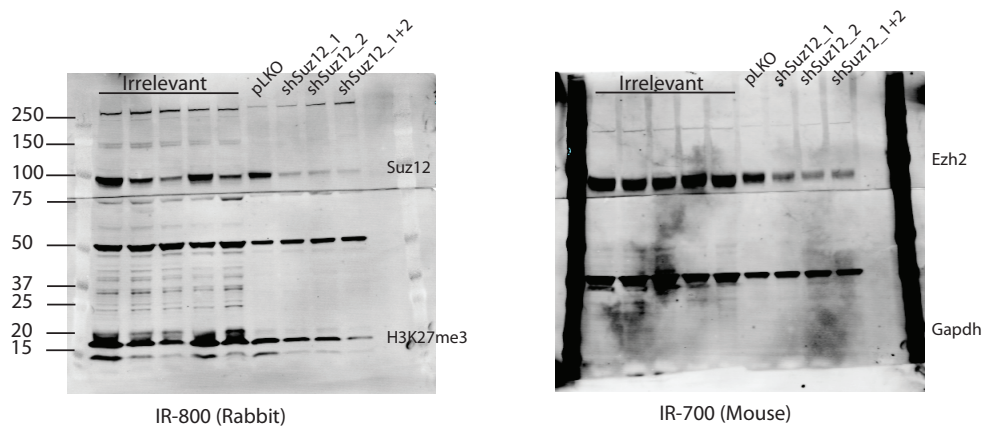
Supplementary Figure 9. Uncropped Western Blots of Key Data

(A) Uncropped gels shown in Figure 1A. Western blot for levels of Brg and pluripotency markers Oct4, Soz2 and Nanog, with GapdH as the loading control. Western blots are performed on the LiCOR Odessey platform with secondary antibodies that emit in the far-red spectrum. Hence, the same blot is scanned twice in different channels (700 and 800), with the 700 channel detecting mouse primary antibodies and the 800 channel depicting anti rabbit primary antibodies. This is consistent throughout the rest of this supplementary document where Western blots are depicted, unless otherwise stated.

(B) Uncropped gels shown in Figure 1D. Western blot depicting STAT3 Protein levels in WT versus KO ESCs (72 hours 4OHT STAT3P=Phosphotyrosine705 STAT3; LIFR=LIF receptor) in the presence of LIF (+) or after 18 hours of LIF starvation (-).

(C) Uncropped gels shown in Figure 1E. Timecourse of STAT3 activation in BrgWT and KO ESCs. Cells were starved for 18 hours from LIF (-), followed by LIF restimuation for the indicated durations. Protein for Brg WT and KO ESC timecourse was run on separate gels because of space constraints. However, since all comparisons of Stat3 phosphorylation dynamics are performed within each gel, this does not pose as a problem.

(D) Uncropped gels shown in Figure S5E. Western blot of PRC2 components Suz12 and Ezh2 in BrgWT and BrgKO ESCs, with GAPDH as a loading control. The relevant lanes are labeled WT and KO. All other lanes pertain to other experimental conditions and are irrelevant here.

(E) Uncropped gels shown in Figure S5F. Western blot of global levels of trimethylated H3K27 (H3K27me3) in soluble fractions of BrgWT and BrgKO ESCs. Hsp90 is used as a loading control.

(F) Uncropped gels shown in Figure S8. Western blots depicting the levels of Polycomb components Suz12, Ezh2 and H3K27me3 after knockdown of Suz12 with 2 distinct shRNA constructs either individually or together. Gapdh is used as a loading control. Certain lanes pertain to different experimental conditions and are labeled as 'irrelevant' here.

Supplementary Table 1. List of Brg and STAT3 CoBound CoActivated Genes These genes are derived from a combination of lower right corner (four squares) of 2D matrix in Figure 1D and also genes with known or suggested roles in ESC self-renewal that are Brg bound, whose transcription depend on Brg and LIF, and are bound by STAT3 using Chen et al.'s STAT3 dataset[3], but were under the peak calling threshold for our STAT3 dataset.

RefSeq	Chr	GeneName	Gene Symbol
NM_010164	chr1	eyes absent 1 homolog (Drosophila)	Eya1
AK143960	chr1	transcription factor CP2-like 1	Tcfcp2l1
NM_021610	chr1	glycoprotein A33 (transmembrane)	Gpa33
NM_175460	chr1	nicotinamide nucleotide adenylyltransferase 2	Nmnat2
BC094606	chr1	formin 2 /// similar to formin-2	Fmn2 /// LOC100044570
NM_027188	chr1	SET and MYND domain containing 3	Smyd3
AK008784	chr1	glycoprotein A33 (transmembrane)	Gpa33
NM_001033193	chr1	frizzled homolog 5 (Drosophila)	Fzd5
NM_013508	chr10	ELK3, member of ETS oncogene family	Elk3
NM_013769	chr10	tight junction protein 3	Tjp3
NM_008635	chr10	microtubule-associated protein 7	Mtap7
NM_007731	chr10	collagen, type XIII, alpha 1	Col13a1
NM_172549	chr10	calcineurin binding protein 1	Cabin1
NM_183426	chr10	strawberry notch homolog 2 (Drosophila)	Sbno2
NM_172496	chr11	cordon-bleu, Cobl	Cobl
BC092257	chr11	voltage-dependent anion channel 1	Vdac1
NM_008686	chr11	nuclear factor, erythroid derived 2,-like 1	Nfe2l1
NM_007707	chr11	suppressor of cytokine signaling 3	Socs3
NM_009242	chr11	secreted acidic cysteine rich glycoprotein	Sparc
NM_013415	chr11	ATPase, Na+/K+ transporting, beta 2 polypeptide	Atp1b2
NM_008750	chr11	nucleoredoxin	Nxn
AK149766	chr11	guanine nucleotide binding protein, alpha 13	Gna13
NM_018861	chr11	solute carrier family 1 (glutamate/neutral amino acid transporter), member 4	Slc1a4
NM_145438	chr11	lethal giant larvae homolog 2 (Drosophila) /// similar to Lethal giant larvae homolog 2 (Drosophila)	Llgl2 /// LOC100047332
NM_011640	chr11	transformation related protein 53	Trp53
AJ297973	chr11	transformation related protein 53	Trp53
AK079604	chr11	acyl-Coenzyme A binding domain containing 4	Acbd4
AK011851	chr11	guanine nucleotide binding protein, alpha 13	Gna13
AK035813	chr11	nuclear receptor co-repressor 1	Ncor1
NM_198861	chr11	cDNA sequence BC046404	BC046404
NM_176902	chr11	family with sequence similarity 100, member B	Fam100b
BC010216	chr11	retinoic acid receptor, alpha	Rara
BC005766	chr11	SEC14-like 1 (S. cerevisiae)	Sec14l1
NM_198292	chr11	testis expressed gene 2	Tex2
NM_028777	chr11	SEC14-like 1 (S. cerevisiae)	Sec14l1

NM_001004144	chr11	G protein-coupled receptor kinase-interactor 1	Git1
NM_011934	chr12	estrogen related receptor, beta	Esrrb
NM_172584	chr12	inositol 1,3,4-triphosphate 5/6 kinase	Itpk1
NM_053122	chr12	IMP2 inner mitochondrial membrane peptidase-like (S. cerevisiae)	Immp2l
NM_011934	chr12	estrogen related receptor, beta	Esrrb
NM_134156	chr12	actinin, alpha 1	Actn1
NM_030172	chr12	RIKEN cDNA 2610021K21 gene	2610021K21Rik
NM_009337	chr12	T-cell lymphoma breakpoint 1	Tcl1
NM_019703	chr13	phosphofructokinase, platelet	Pfkp
U68182	chr13	glucosaminyl (N-acetyl) transferase 2, I-branching enzyme	Gcnt2
AK019924	chr13	glucosaminyl (N-acetyl) transferase 2, I-branching enzyme	Gcnt2
AK136428	chr14	solute carrier family 15 (oligopeptide transporter), member 1	Slc15a1
NM_001033336	chr14	ATP-binding cassette, sub-family C (CFTR/MRP), member 4	Abcc4
NM_030255	chr15	apolipoprotein B mRNA editing enzyme, catalytic polypeptide 3	Apobec3
BC004728	chr15	cDNA sequence BC004728	BC004728
NM_145930	chr15	expressed sequence AW549877	AW549877
NM_001033274	chr15	bromodomain containing 1 /// similar to bromodomain containing 1	Brd1 /// LOC100045983
NM_025842	chr15	vacuolar protein sorting 28 (yeast)	Vps28
NM_130859	chr15	caspase recruitment domain family, member 10	Card10
NM_172607	chr15	nicotinate phosphoribosyltransferase domain containing 1	Naprt1
NM_001004150	chr15	alpha 1,4-galactosyltransferase	A4galt
NM_009893	chr16	chordin	Chrd
NM_013790	chr16	ATP-binding cassette, sub-family C (CFTR/MRP), member 5	Abcc5
NM_009744	chr16	B-cell leukemia/lymphoma 6	Bcl6
NM_009379	chr16	thrombopoietin	Thpo
NM_008480	chr17	laminin, alpha 1	Lama1
BC068268	chr17	POU domain, class 5, transcription factor 1	Pou5f1
NM_026644	chr17	1-acylglycerol-3-phosphate O-acyltransferase 4 (lysophosphatidic acid acyltransferase, delta)	Agpat4
NM_027366	chr17	lymphocyte antigen 6 complex, locus G6E	Ly6g6e
NM_008738	chr17	neurturin	Nrtn
NM_008804	chr17	phosphodiesterase 9A	Pde9a
NM_026530	chr17	MPN domain containing	Mpnd
NM_022880	chr17	Solute carrier family 29 member 1)	Slc29a1
NM_146090	chr18	zinc binding alcohol dehydrogenase, domain containing 2	Zadh2
NM_008137	chr19	guanine nucleotide binding protein, alpha 14	Gna14
NM_145123	chr19	cartilage acidic protein 1	Crtac1
NM_010324	chr19	glutamate oxaloacetate transaminase 1, soluble	Got1

NM_009037	chr2	reticulocalbin 1	Rcn1
NM_008652	chr2	myeloblastosis oncogene-like 2	Mybl2
NM_021606	chr2	NIMA (never in mitosis gene a)-related expressed kinase 6	Nek6
NM_177343	chr2	calcium/calmodulin-dependent protein kinase ID	Camk1d
NM_146128	chr2	discs, large homolog-associated protein 4 (Drosophila)	Dlgap4
NM_146119	chr2	family with sequence similarity 129, member B	Fam129b
BC060121	chr2	PHD finger protein 20	Phf20
NM_028072	chr2	sulfatase 2	Sulf2
NM_172661	chr2	HLA-B associated transcript 2-like	Bat2l
NM_172475	chr2	FERM domain containing 4A	Frmd4a
NM_027941	chr3	leucine rich repeat containing 34	Lrrc34
NM_008857	chr3	protein kinase C, iota	Prkci
NM_133218	chr3	zinc finger protein 704	Zfp704
BC100519	chr3	leucine rich repeat containing 34	Lrrc34
NM_027241	chr3	polymerase (RNA) III (DNA directed) polypeptide G like	Polr3gl
AK015024	chr3	leucine-rich repeats and IQ motif containing 4	Lrriq4
NM_133754	chr4	filamin binding LIM protein 1	Fblim1
NM_010174	chr4	fatty acid binding protein 3, muscle and heart	Fabp3
NM_008126	chr4	gap junction protein, beta 3	Gjb3
NM_080555	chr4	phosphatidic acid phosphatase type 2B	Ppap2b
NM_009736	chr4	BCL2-associated athanogene 1	Bag1
NM_146155	chr4	AT hook, DNA binding motif, containing 1	Ahdc1
NM_026257	chr4	UBX domain protein 11	Ubxn11
NM_011385	chr4	ski sarcoma viral oncogene homolog (avian)	Ski
AK137588	chr4	WW domain containing E3 ubiquitin protein ligase 1	Wwp1
NM_144531	chr4	RIKEN cDNA 9030409G11 gene	9030409G11Rik
NM_172383	chr4	transmembrane protein 125	Tmem125
NM_173426	chr4	family with sequence similarity 110, member B	Fam110b
NM_177733	chr4	E2F transcription factor 2	E2f2
NM_009642	chr4	angiotensin II, type I receptor-associated protein	Agtrap
NM_009469	chr5	Unc-51 like kinase 1 (C. elegans)	Ulk1
NM_178446	chr5	RNA binding motif protein 47	Rbm47
NM_198602	chr5	cut-like homeobox 1	Cux1
NM_175423	chr5	ORAI calcium release-activated calcium modulator 1	Orai1
NM_194344	chr5	SH3 domain and tetratricopeptide repeats 1	Sh3tc1
NM_172723	chr5	ArfGAP with dual PH domains 1	Adap1
NM_011535	chr5	T-box 3	Tbx3
AK146829	chr5	procollagen C-endopeptidase enhancer protein	Pcolce
NM_007646	chr5	CD38 antigen	Cd38
NM_024434	chr5	leucine aminopeptidase 3	Lap3

AF343349	chr5	general transcription factor II I repeat domain-containing 1	Gtf2ird1
NM_013535	chr6	gene rich cluster, C10 gene	Grcc10
AK162776	chr6	solute carrier family 6 (neurotransmitter transporter, taurine), member 6	Slc6a6
NM_013820	chr6	hexokinase 2	Hk2
NM_197985	chr6	adiponectin receptor 2	Adipor2
NM_011708	chr6	Von Willebrand factor homolog	Vwf
NM_009320	chr6	solute carrier family 6 (neurotransmitter transporter, taurine), member 6	Slc6a6
NM_015829	chr6	solute carrier family 25 (mitochondrial carrier, adenine nucleotide translocator), member 13	Slc25a13
NM_009795	chr7	calpain, small subunit 1	Capns1
NM_027898	chr7	GRAM domain containing 1A	Gramd1a
NM_016721	chr7	IQ motif containing GTPase activating protein 1	Iqgap1
NM_008803	chr7	phosphodiesterase 8A	Pde8a
AF191090	chr7	nephrosis 1 homolog, nephrin (human)	Nphs1
NM_009980	chr7	C-terminal binding protein 2	Ctbp2
NM_144522	chr7	TBC1 domain family, member 10b	Tbc1d10b
BC009088	chr7	poliovirus receptor-related 2	Pvrl2
NM_145149	chr7	RAS guanyl releasing protein 4	Rasgrp4
NM_009795	chr7	calpain, small subunit 1	Capns1
NM_144529	chr7	Rho GTPase activating protein 17	Arhgap17
NM_027470	chr7	p21 protein (Cdc42/Rac)-activated kinase 4	Pak4
NM_029660	chr7	similar to testes-specific heterogenous nuclear ribonucleoprotein G-T /// RNA binding motif protein, X-linked-like 2	LOC10004643 3 /// Rbmxl2
AK029434	chr7	IQ motif containing GTPase activating protein 1	Iqgap1
NM_175433	chr7	zinc finger protein 710	Zfp710
NM_175433	chr7	zinc finger protein 710	Zfp710
NM_016754	chr7	myosin light chain, phosphorylatable, fast skeletal muscle	Mylpf
NM_019573	chr8	WW domain-containing oxidoreductase	Wwox
NM_133255	chr8	hook homolog 2 (Drosophila)	Hook2
NM_146217	chr8	alanyl-tRNA synthetase	Aars
NM_025768	chr8	GH regulated TBC protein 1	Grtp1
NM_008624	chr9	muscle and microspikes RAS	Mras
NM_011176	chr9	suppression of tumorigenicity 14 (colon carcinoma)	St14
NM_009389	chr9	transducin-like enhancer of split 3, homolog of Drosophila E(spl)	Tle3
NM_008542	chr9	MAD homolog 6 (Drosophila)	Smad6
NM_026036	chr9	CKLF-like MARVEL transmembrane domain containing 6	Cmtm6
NM_144937	chr9	ubiquitin specific peptidase 3	Usp3
NM_028838	chr9	leucine rich repeat containing 2	Lrrc2
BC058971	chr9	trafficking protein, kinesin binding 1	Trak1
NM_173781	chr9	RAB6B, member RAS oncogene family	Rab6b
BC024389	chr9	muscle and microspikes RAS	Mras

Supplementary Table 2. List of Primers Used In this study

RT-PCR Primers for Transcript Analysis

Gene	Forward	Reverse
gap junction protein, beta 3, Gjb3	GAATCAAGGCCAGGTCTGAG	ATGCCGTGGAGTACTGGTTC
laminin, alpha 1, Lama1	GATCCCATTTATGTGGGTGG	CTTGTAGGTCAAAGGCTCGG
muscle and microspikes RAS, Mras	AGAGACCAGTGCCAAGGACC	TCAGTGCAGTTAGGCAGTGG
angiotensin II, type I receptor-associated protein, Agtrap	CTACCACATGCACCGTGAAC	CCAGGGACAGCTTCAGTACC
eyes absent 1 homolog (Drosophila), Eya1	GTGTGGAAGAAGAGCAAGGG	CAAGCCTGCTGGGTTATCTC
fatty acid binding protein 3, muscle and heart, Fabp3	GCAAACTCATCCATGTGCAG	TCAGAGGGGAAAACCATGAG
estrogen related receptor, beta, Esrrb	GGTGCGCAGGTACAAGAAAC	AGGAAGAGTTTGTGCATGGG
junction adhesion molecule 2, Jam2	GGGCAGTCCTGCATCTAAAG	TTTGGTGCAGCTCAAAACTG
lymphocyte antigen 6 complex, locus G6E, Ly6g6e	TGTTACACCTGCAGCTTTGC	TGCATAGGTCCTGCTCACAG
leucine rich repeat containing 34, Lrrc34	TTGCACTTTCCCAGTCAATG	TTTCTCCATAAGTCGGTGCC
filamin binding LIM protein 1, Fblim1	AAAATCGAGTGCATGGGAAG	AGAGGTGGTCATTCAGTGGG
cordon-bleu, Cobl	AGACAAGCCTTGATGGATGC	CGCCACTTCTTGAAGGTTTC
inositol 1,3,4-triphosphate 5/6 kinase, Itpk1	TCATTAACAACCAGACCGGG	GGTCTCAGTCTTCCAGGGTG
phosphofructokinase, platelet, Pfkp	TGTTTCAACCAGTGGCAGAG	TGGCAGACTTGATGAGATGG
calpain, small subunit 1, Capns1	CCGGACAGATCCAAGTGAAC	TGGCTCCATAGTGAGCTGTG
T-box 3, Tbx3	CTACGGGGGAGCAATGGATG	AGTTTAGTATAGTAAATCCG
T-cell lymphoma breakpoint 1, Tcl1	ACCTTGGGGGAAGCTATGTC	CTTGGAGCCCAGTGTAGAGG
phosphatidic acid phosphatase type 2B	GCCTTCTACACGGGATTGTC	TGTTCCTGTCGATGATGTCC
Solute carrier family 29 member 1	GGAGCCTCACTGCTGTCTG	TGATGTTTCCTGCTGTCTCC

ChIP Primers for STAT3 Site and DnaseI Assay

Gene	Forward	Reverse
gap junction protein, beta 3, Gjb3	CTCAGACCTGGCCTTGATTC	GACAGGCAGATGATAAATGGG
laminin, alpha 1, Lama1	AGCTCCAAGAAAGGAGGGAC	AGGATGCTTCCCTGAAATCC
muscle and microspikes RAS, Mras	TTTCTAAGTAAAGCCGGCCC	GGAATTGTGCAGAAGGGAAG
angiotensin II, type I receptor-associated protein, Agtrap	GCCTCAGTTTCCCTCTCTTTG	GAAGAGAGTCCCCCATAGCC
eyes absent 1 homolog (Drosophila), Eya1	CTGAGAAAGTCTGGCCAAGG	ACTCACTGCCATTCCTCCTG
fatty acid binding protein 3, muscle and heart, Fabp3	CCGGAAGAACCCTCTGAATAG	GAGAACGTGACCTTGCTTCC
estrogen related receptor, beta, Esrrb	ATGTTTACCCCCTCTGTCCC	AAGGCTTTGTCCTCTTTGCC
junction adhesion molecule 2, Jam2	GAGCACAAAAGAAAGCCAGC	AGATGACCTTGCTTCCTCCC
lymphocyte antigen 6 complex, locus G6E, Ly6g6e	TGAATCAAAGGCATGTGAGC	GCTGTTCCCGGTTCTAGTTG
leucine rich repeat containing 34, Lrrc34	TGGAACACCAGCACTAATGG	TGATAAAGGAGGGAACACCG
filamin binding LIM protein 1, Fblim1	ATCCAAACCAGTTTCTTGCG	CTGCATGACAACGTAAAGGG
cordon-bleu, Cobl	TTTAAGTGCTGAGGGGTTGG	TCTTCCCCTCACTATGTGCC
inositol 1,3,4-triphosphate 5/6 kinase, Itpk1	GACCGTTCTTCTCCACAAGC	CCTCTTTCCCCATGACCCTA
phosphofructokinase, platelet, Pfkp	CCGGAGTTCCTCTTCAATCC	AGAACCCTGCTAAGGCAAGA
calpain, small subunit 1, Capns1	TGCCTCCTCACCAGCTACTT	ACTTGCTGACAGGGTGGAAC
T-box 3	CTCAATTCTCTGCCCTTTGG	CAGCCAGTGAAGGTGCTTG
T-cell lymphoma breakpoint 1, Tcl1	GGAGTCACCCTCATTTCCAG	CCCTTTCCTCTTTCCTTTTTG
phosphatidic acid phosphatase type 2B	CAGCAGTCTTTCCTGGTTTTC	TGTGTGGACTTGGGTGTGTC
Solute carrier family 29 member 1	CTAGGGCCTTTTCCAGAACC	GCTCCCTTGTGATGTCCAGT
myeloid leukemia factor 1 interacting protein, Mlf1ip	AGCAATGCGAAGGATTTGAC	CCTGGAAAACACCCAACAG
SWI/SNF-related matrix-associated actin-dependent regulator of chromatin subfamily D member 2 , Smarcd2	CGGGACTTCCCGATTTTACT	TAACCGCCTCTGGGTAACTG
teratocarcinoma-derived growth factor, Tdgf	TCCAGCCACTTTTCCAGTTC	AAGGTGTCGCCCTCCTAATC
immediate early response 2, Ier2	TCCAGTTAACCCAGGACACC	CCCAAGGGTTGGACTAGAGAG
sprouty homolog 2, Spry2	TTCAAACCCTGGACAAAAGG	GAAGGCCCACAGAAACAAAG
ubiquitin specific protease 3, Usp3	CTCCGGAGAACGTGAAAATC	ACTTCACATCCCCGTAGGAC

Thyroid specific PTB domain protein homolo,Tns3	ATAAGCTGACGCCACCAAAG	GTAGCCGGGAGCTACACATC

ChIP Primers for Promoters of STAT3/Brg Dependent Genes	**Forward**	**Reverse**
gap junction protein, beta 3, Gjb3	CTCAGACCTGGCCTTGATTC	CAGGAACAGACTGACCAGGG
laminin, alpha 1, Lama1	GAACAGATCCCCTTGGGAAG	GAGTGTGCTCTTCCCAGCTC
muscle and microspikes RAS, Mras	GACGCCTTAAAGCGACCG	ACAGACTGCAGATCCGTGTG
angiotensin II, type I receptor-associated protein, Agtrap	TAGGCTCAGGCTCCTGCTAC	TCACCTCGATCCCACTTAGG
eyes absent 1 homolog (Drosophila), Eya1	TTGTTTTGTTTTTGCAACGC	TCCCCCACAGCTGTTTATTC
fatty acid binding protein 3, muscle and heart, Fabp3	CGGTACCTGGAAGCTAGTGG	CTGGACTGGCTAGGAGCTTG
estrogen related receptor, beta, Esrrb	CAGCCTTCCTACTCCACAGG	AGTGACAGAATCGAGCTGGG
junction adhesion molecule 2, Jam2	GAGGAGAGACATGGCGAGAC	AAGGGTGGAAGAGGGTTGAG
lymphocyte antigen 6 complex, locus G6E, Ly6g6e	CTAGAACCGGGAACAGCTTG	CTTGCCTTGAGGGTCTTCTG
leucine rich repeat containing 34, Lrrc34	CTCTCCTCACGAAGACAGGG	GGAGCGACTCTGGTTACTGG
filamin binding LIM protein 1, Fblim1	CTGTGAGGTTCCCACTCTCC	CCCTCAAGCTCCTGCTACAC
cordon-bleu, Cobl	TCCTCATTCACTTTTTCCGC	GTCCGTCTCTCTCCGCAC
phosphatidic acid phosphatase type 2B, Ppap2b	GCTCAGAAAACAAACCGAGC	TCCTGCAGCTAGCTCTCCTC
inositol 1,3,4-triphosphate 5/6 kinase, Itpk1	CTCCTCACCTGCACAGCTC	GCCGAGGAGGAAGAAGATG
phosphofructokinase, platelet, Pfkp	ACCAGCGAGAGAGCTGGTAG	CGAAGTACCTGGAGCACCTC
calpain, small subunit 1, Capns1	ACTGGAGTGTCCCGTCTCAC	TGCAATGGAGGCTCTAGGAC

Supplemental Methods

Culture of ES cells

ESCs were cultured in Knockout Dulbecco's modified eagle medium (Gibco, Cat# 10829) supplemented with 7.5% ES-qualified FBS (Invitrogen, Cat#16141-079), 7.5% Knockout Serum Replacement (Invitrogen, Cat#10828028), 2mM L-glutamine (Gibco #25030-081), 10mM HEPES (Gibco #15630-080), 100U/ml penicillin/streptomycin (Gibco #15070-063), 0.1mM non-essential amino acids (Gibco #11140-050), 0.1mM beta-mercaptoethanol (Gibco #21985-023) and 1000U/ml LIF (Esgro, Chemicon #ESG1107). ES cells were maintained at 37°C, 7% carbon dioxide, fed with fresh media daily, and passaged onto new plates following trypsin dissociation.

Generation of Brg^{cond} ESCs and Induction of Brg Deletion

Day 3.5 blastocysts were flushed from oviducts of Brg^{lox/lox} female mice [4](of mixed background) to Brg^{lox/lox}; Actin-CreER male mice. The zona pellucida was removed by Acid Tyrode's solution (Sigma) and embyroes were cultured on MEFs in ES media (15% Knockout serum replacement and 3000U/ml ESGRO LIF). After 5-6 days of culture, inner cell mass outgrowths from the embryos were dissociated by trypsin digestion and passaged onto MEF feeders. Single colonies were picked from these bulk cultures, expanded and genotyped to obtain Brg^{lox/lox}; Actin-CreER ESC clones, or Brg^{cond} ESCs. We performed all our experiments with line 6-14, which was karyotypically normal and grew well both with MEF feeders or in feeder-free conditions on gelatinized culture dishes. To induce *Brg* deletion in these lines, we treated the cultures grown on MEFs with 1uM 4-hydroxytamoxifen (4-OHT Sigma, dissolved in ethanol) for 24 hours, then passaged them onto gelatinized plates for 48 more hours of 4-OHT treatment. As a control, 6-14 Brg^{cond} cells were treated with ethanol, which does not induce Cre expression.

DnaseI Hypersensitive Assay

This assay to measure DNA accessibility was performed according to [5]. Briefly, ESCs were grown on feeder-free gelatinized culture dishes for 2 days until near confluence. ESCS were lysed with ice-cold DnaseI digestion buffer (10mM Hepes pH7.6, 50mM KCl,

5mM MgCl$_2$, 3mM CaCl$_2$, 0.1% NP-40, 8% glycerol, 1mM DTT), scraped from the plate and disrupted with 4 strokes of a dounce homogenizer to isolate single nuclei. The nuclei were stained with trypan blue, counted and resuspended to a concentraion of 12.5E6/ml. 2.5E6 cells were used for each DNaseI reaction. Increasing amounts of DNaseI (Worthington) (from 0U/10E6 cells to 15U/10E6 cells) was added to each reaction one at a time, mixed and incubated at 37°C for exactly 3 minutes. The reaction was immediately terminated by addition of equal volume of DNase Stop buffer (1% SDS, 15mM EGTA). The samples were then incubated with RnaseA (Invitrogen) for 1 hour at 37°C , followed by Proteinase K (Invitrogen) overnight at 55°C. An equal amount of *Drosophila* genomic DNA (from S2 cells) was spiked into each reaction to add as internal loading control to minimize variations arising from the phenol-chloroform extraction procedure. DNA was then extracted by phenol-chloroform extraction, resuspended in 60ul of Tris-EDTA. The undigested input sample was then briefly sonicated to solubilize it to enable more accurate pipetting. Each sample was diluted 30-fold and 1 ul used as input for QPCR reaction. QPCR was performed with primers spanning STAT3 binding sites or control regions. A S2-specific primer set as used as an internal control. Target sites were chosen from genes in Table S1 and are the same gene set used in ChIP assays throughout the manuscript. DnaseI accessibility for each sample was then calculated as:

$$\left[\left(\frac{Test\_Amplicon}{S2\_Amplicon}\right)_{Digested} \div \left(\frac{Test\_Amplicon}{S2\_Amplicon}\right)_{Undigested\_Input}\right] \times 100\%$$

STAT3 Activation

To manipulate the LIF signaling pathway, Brg[cond] cells were grown on MEF feeders in LIF-containing ES media and then passaged onto gelatin coated plates in ES media not containing LIF for the indicated amount of time before harvesting for experiments.

Extraction of RNA

RNA was extracted using Trizol reagent (Invitrogen), followed by RNeasy kit with DNaseI digestion to eliminate genomic DNA.

Chromatin ImmunoPrecipitation (ChIP)

ChIP experiments were performed with EZ-ChIP (Millipore) with antibodies listed below. Brg^{cond} ESCs were grown on gelatinized culture dishes for 2-3 days. ESCs were fixed on-plate with 1% formaldehyde in PBS for 12 minutes, the reaction quenched with 0.125M glycine for 5 minutes on ice, and the cells were washed 2X with ice-cold PBS containing protease inhibitors and then scraped from the plates in PBS. 10E7 pelleted cells were resuspended in 1ml ChIP buffer (0.1% SDS, 1mM EDTA, 20mM Tris-HCL pH 8.1, 150mM NaCl, 0.1% Triton-X100) and sonicated for 9-10 cycles, 30 seconds per cycle with 60 seconds' rest between each cycle, at Power 6 on the Misonix Sonicator 3000. ChIP lysates centrifuged at 13000rpm for 5 minutes at 4C to remove any insoluble material. The supernatant was then diluted to a protein concentration of 1.7mg/ml and 350-500ug of protein was used for each immunoprecipitation reaction after preclearing with the Agarose A/G beads (Millipore). Antibodies were routinely used at a concentration of 1ug per 100ug of ChIP lysate, or at 1:50 dilution for Cell Signaling antibodies. Immunoprecipitation was performed at 4C overnight with constant gentle inversion. The beads were then washed once (5 minutes per wash, with gentle inversion at 4C) in succession with 1ml of each of the following buffers : (1) Low Salt Buffer (2) High Salt Buffer; (3) LiCl Buffer; (4) TE; (5) Water, then eluted twice with 250ul of elution buffer (1mM NaHCO$_3$ and 1% SDS). The DNA was subsequently reverse-crosslinked by incubating at 65C overnight in the presence of 0.04M NaCl, and digested with Proteinase K for 2 hours at 55C. ChIP DNA was extracted by phenol-chloroform extraction and resuspended in 60 ul of TE. 1ul was used for each QPCR reaction.

Antibodies Used in This Study. Table 1.1 lists the antibodies that were used in this study for ChIP assays.

Antibody	Company	Clone
Brg	Crabtree Lab	J1
STAT3	Santa Cruz	C20X
STAT3-pT705	Cell Signaling	D3A7
STAT3-pS727	Santa Cruz	sc-135649
Oct4	Santa Cruz	sc-9081
Sox2	Santa Cruz	sc-17319
Nanog	Bethyl Laboratories	A300-398A

LIFR	Santa Cruz	sc-659
Gp130	Santa Cruz	sc-655
H3K27me3	Millipore	07-449

Datasets used in this study

ChIP-seq datasets from mESCs were obtained from [6], [3] and [7].

ChIP-Seq and Peak Calling

Sequenced 36-bp reads from STAT3 ChIP-Seq experiments were mapped to the mouse genome (mm8 assembly) using the Solexa Analysis Pipeline. Only those reads that mapped to unique genomic locations with at most two mismatches were retained for further analysis. This resulted in 13.4 and 12.6 million reads for STAT3 ChIP and 53.9 and 51.2 million reads for H3K27me3 in WT and Brg KO cells, respectively. For control, input DNA libraries were sequenced in both WT and Brg KO cells yielding a net 14.3 and 14.5 million reads, respectively. STAT3 and the input DNA reads were processed further using the SISSRs tool [8] to identify STAT3 binding sites in WT and Brg KO cells. SISSRs was run with -a and other default options with p-value threshold set to 0.01. A total of 2729 and 545 STAT3 binding sites were detected in WT and Brg KO cells. Of the 2729 STAT3 sites in WT, 442 were also detected to bind STAT3 in Brg KO cells (referred to as Brg-dependent STAT3 sites). The remaining 2287 STAT3 sites in WT, which were lost upon Brg KO, were considered as Brg-independent STAT3 sites. ChIP-seq reads for Brg and input DNA in E14 WT ES cells, obtained from our previous study (Ho et al., 2009a), was reanalyzed using a more stringent approach (as described in Visel et al., Nature 2009, PMID: 19212405) to define Brg binding regions (peaks). In brief, the 25-bp reads were extended to 300bp in the 3' direction to account for the average 300bp length ChIP DNA fragments size-selected for sequencing. The read coverage at individual nucleotides at 20bp resolution was determined by counting the number of extended reads that map to 20bp intervals. Brg binding regions were identified by comparing the observed frequency of coverage depths with those expected from a random distribution of the same number of reads. The probability of observing a Brg peak with a coverage depth of atleast R by chance is given by a sum of Poisson probabilities as

$$1 - \sum_{n=0}^{R-1} \frac{e^{-\lambda}\lambda^n}{n!}$$

where λ is the average genome-wide coverage of extended reads. The mappable genome length which was estimated to be about 80% of the genome, and the smallest coverage depth T at which the ratio of the expected number of sites with at least that coverage to the observed number is at most 0.01 was determined (FDR≤0.01). Candidate Brg peaks were identified by selecting sites at which the read coverage exceed T, and the peak boundaries were extended to the nearest flanking position at which the read coverage fell below two reads. Overlapping peaks were merged into a single peak. Consecutive Peaks separated by 2 times the average ChIP DNA fragment size were merged into a single peak as well. The latter was performed to account for regions with lack of coverage depth. Peaks mapping to satellite repeats, ribosomal RNA repeats and those that have also been reported as peaks in the control input DNA sample were discarded. The remaining 10,829 peaks were considered to be the high-confidence Brg binding regions. Although the number of Brg binding regions identified in this manner is similar in number to Brg islands we had reported previously (Ho et al., 2009a), the median width of the Brg bound regions identified as described above is 700bp compared to 6.5Kb that we had reported previously (Ho et al., 2009a). The main reason for this difference is that the strategy outlined above for identifying binding regions helped reduce the number of false-positives (compared to our previous approach) and at the same time increased the resolution of the identified binding regions by breaking up previously defined large Brg binding islands. All of our results reported in this study as well as those in our previous study (Ho et al, 2009a) remain the same regardless of whether we use Brg binding regions defined in this study or Brg islands defined in our previous study (data not shown).

Target Gene Assignment

Throughout the manuscript, direct target genes of a particular factor (e.g STAT3 or Brg) are defined as genes that have one more more detected factor peak(s) by ChIP-seq analysis within 5Kb upstream of the transcription start site (TSS) to the end of the gene (TES).

Microarray Data Analysis

Purified RNA was processed and hybridized onto Affymetrix Mouse MOE4.0 3'
expression arrays according to the manufacturer's instructions (Affymetrix Inc.). The
data were then normalized and summarized using Affymetrix's Expression Console™
Software with the RMA algorithm. Inter-array comparisons were performed using
modules available at GenePattern (Broad Institute, www.genepattern.org). First, the
preprocess dataset module was used to keep probesets with absolute intensity readings
in the range of 20-20000, to avoid spurious large fold changes associated with very
lowly expressed genes (i.e. <20), and to avoid probesets that had reached saturation (i.e.
>20000). Subsequently, the Comparative Marker Selection module was utilized to select
probe sets that were significantly changed between two conditions using a 2-sided T-
test with 1000 permutations as the statistical test.

Generation of 2D Matrices and Gene Density Heatmap

The 17,030 UCSC known genes with expression data in ES cells, obtained from a published
microarray data of wildtype E14 ES cells [1], were grouped into 10 bins based on expression.
To study Brg's role in LIF/STAT3 signaling in ES cells, we first computed the fold change
for 17,030 known genes in Brg KO compared to the WT ES cells. To avoid including genes
with artificial fold changes (nil to negligible or vice-versa), we removed ~15% of the genes
with lowest expression levels in both the WT and the KO/KD samples. The resulting genes
from each dataset were then grouped into 10 bins based on the fold change. Using the same
strategy, we also grouped genes into 10 bins based on the fold change in ES cells with and
without LIF, embryoid body (EB) cells compared to ES cells [9]. The relationship between 2
datasets (10-bin sets) was assessed by performing pairwise comparisons of bins from the 2
datasets, and counting the number of genes in common between every pair of bins. The
resultant matrix containing the number of common genes was plotted as a gene density heat
map to infer the interplay between the functional roles between Brg and LIF/STAT3.

STAT3 Motif Analysis

MEME [10] was used to identify sequence motifs within STAT3 binding sites.

Determining overlap between ChIP-seq datasets

Overlap between ChIP-seq peaks from two different datasets was required for counting physical overlap. For gene target counts, alternative splice forms were collapsed into genes according to annotations for mouse genome build mm8 from the UCSC Genome Browser (http://genome.ucsc.edu/). Venn diagrams were constructed using the Area-Proportional Venn Diagram Plotter and Editor from Bio-Info Management (http://bioinfoman.com/free/bxarrays/venndiagram.php).

References

1. Loh, Y. *et al.* The Oct4 and Nanog transcription network regulates pluripotency in mouse embryonic stem cells. *Nat Genet* **38**, 431-440 (2006).
2. Masui, S. *et al.* Pluripotency governed by Sox2 via regulation of Oct3/4 expression in mouse embryonic stem cells. *Nat Cell Biol* **9**, 625-635 (2007).
3. Chen, X. *et al.* Integration of external signaling pathways with the core transcriptional network in embryonic stem cells. *Cell* **133**, 1106-1117 (2008).
4. Bultman, S. *et al.* A Brg1 null mutation in the mouse reveals functional differences among mammalian SWI/SNF complexes. *Mol Cell* **6**, 1287-1295 (2000).
5. Dorschner, M.O. *et al.* High-throughput localization of functional elements by quantitative chromatin profiling. *Nature methods* **1**, 219-225 (2004).
6. Ho, L. *et al.* An embryonic stem cell chromatin remodeling complex, esBAF, is an essential component of the core pluripotency transcriptional network. *Proceedings of the National Academy of Sciences of the United States of America* **106(13)**, 5187-5191 (2009).
7. Ku, M. *et al.* Genomewide analysis of PRC1 and PRC2 occupancy identifies two classes of bivalent domains. *PLoS Genet* **4**, e1000242 (2008).
8. Jothi, R., Cuddapah, S., Barski, A., Cui, K. & Zhao, K. Genome-wide identification of in vivo protein-DNA binding sites from ChIP-Seq data. *Nucleic acids research* **36**, 5221-5231 (2008).
9. Sene, K. *et al.* Gene function in early mouse embryonic stem cell differentiation. *BMC Genomics* **8**, 85 (2007).
10. Bailey, T.L., Williams, N., Misleh, C. & Li, W.W. MEME: discovering and analyzing DNA and protein sequence motifs. *Nucleic acids research* **34**, W369-373 (2006).